8 Evolution after the AGB

As stated earlier, the evolutionary speed of AGB stars is set by their mass loss, not by their nuclear burning. As AGB stars evolve both their pulsation periods and luminosity increase, and so their mass loss rates also increase (although the exact dependence of $\dot{M}$ on the stellar parameters is not known). The highest known mass loss rates are of the order 10^{-4} $M_{\odot}$ yr^{-1}, but these stars are difficult to study since they are completely obscured at optical and possibly even at near-IR wavelengths. This final phase of extreme mass loss on the AGB is often called the superwind phase.
When the stellar envelope mass drops below a certain, low value ($\sim 10^{-2} - 10^{-3}$ $M_{\odot}$), it can no longer maintain itself in hydrostatic equilibrium, and starts to contract. This is the end of the AGB phase.
The core region does not care about the envelope and keeps the same luminosity as before, and since

$$L = 4\pi R^2 \sigma T_{\rm eff}^4 \tag{74}$$

this means that as the star shrinks, the effective temperature goes up. Plotted in the HR-diagram this phase of the evolution is characterized by a horizontal (constant luminosity) movement towards the blue side of the diagram, see Fig. 38. This blueward evolution continues to very high values of $T_{\rm eff}$, more than 10^5 K, making these stars among the hottest known stars. It stops when the stellar envelope can no longer supply the nuclear burning zone with enough fuel, and nuclear burning stops. At that point the stellar luminosity starts to drop, and the effective temperature slowly starts to go down. This process continues turning the star into a White Dwarf on the so-called White Dwarf cooling track.
This is the general picture of post-AGB evolution. The details depend on various stellar properties

1. Stellar mass
2. Mass loss during the post-AGB phase.
3. Nature of the energy source at the end of the AGB (active H-shell or active He-shell).

which we will look at in the following sections.

8.1 Stellar mass and post-AGB evolution

Just as on the AGB the post-AGB phase has a core mass-luminosity relation, as to a large extent the core is decoupled from the rest of the star. The form of this L–$M_{\rm core}$ relation is

$$L = 5.9 \times 10^5 (M_{\rm core} - 0.522) \quad L_{\odot} \tag{75}$$

(Paczynski 1970). Obviously, lower mass stars have lower luminosity. The core mass also determines the evolutionary speed: the lowest mass (~ 0.5 $M_{\odot}$) stars take 10,000s of years to reach their highest $T_{\rm eff}$, the highest mass stars ($\sim$ 1.2 $M_{\odot}$) do it in $\sim$ 100 years, see Fig. 38.

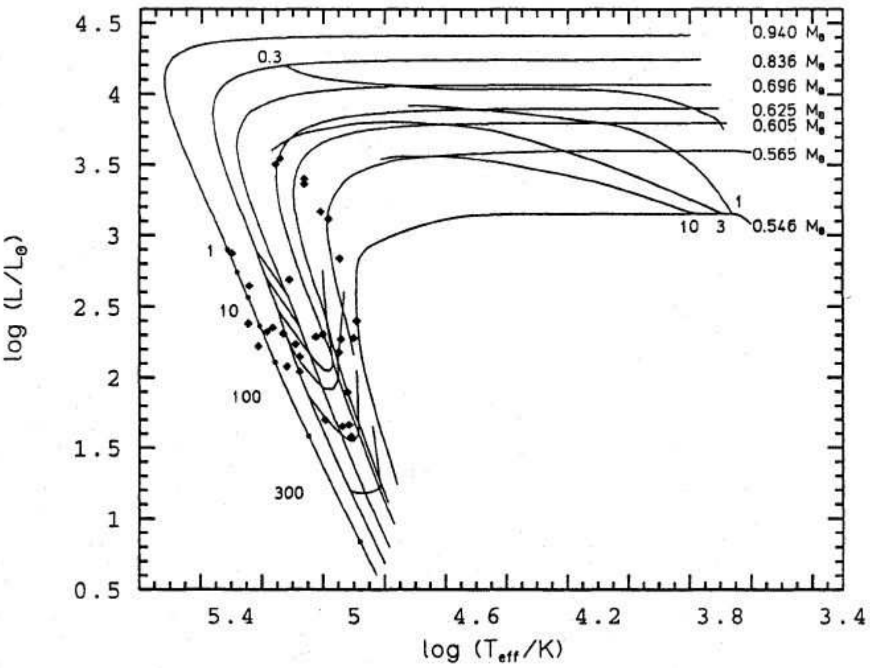

Figure 38: Stellar evolution calculations for a range of (AGB) masses (ndicated at the start of the evolutionary tracks. The lines crossing the tracks connect points of equal post-AGB age in units of 1000 years. The dots are observed post-AGB stars. The pile up of points show that the evolution is slowing down in that part of the diagram. From Blöcker (1995)

8.2 Mass loss during the post-AGB phase

Any mass loss during the post-AGB phase speeds up the evolution, since it will remove additional material from the already thin stellar envelope. Unfortunately for those who want to precisely model post-AGB evolution, the post-AGB mass loss rates are not well known.

Initially, the mass loss process is identical to that on the AGB, but as the stellar photosphere gets hotter, dust production becomes impossible and other mechanisms have to take over. For $T_{\rm eff} > 3 \times 10^4$ K a stellar wind can be driven using radiation pressure on (resonance) lines. This is the same process that drives the mass loss in massive O stars. The theoretically calculated mass loss rates and wind velocities match the observed ones quite closely with typical values of $\dot{M} \sim 10^{-9}$—10^{-7} $M_\odot$ yr^{-1} and wind velocities of 1000—2000 km s^{-1} (Pauldrach et al. 1988). These winds are therefore called 'fast winds'.

Below effective temperatures of 3×10^4 K the situation is unclear. There are observational indications for outflows of typical speeds ~ 100 km s^{-1}, but the mechanism is not understood. The observed outflows are often well collimated into two or more narrow beams. Estimates of the momentum in the outflows indicates that they exceed the limits of radiation-driven winds, even the multiple scattering limit. This has triggered discussions about jet- or bullet-like outflows being launched through magnetic forces from some sort of disc-like structure close to the star. All of this remains very uncertain, see also. Sect. 8.4.3.

8.3 Thermal pulse phase and post-AGB evolution

Depending on during which part of a TP cycle a star leaves the AGB, its main energy source will be the H-shell or the He-shell.

$0 < \phi < 0.15$ He-shell

$0.15 < \phi < 0.3$ H + He-shell (50/50)

$0.3 < \phi < 1$ H-shell ($L_{\rm He} \sim 0.1 L_{\rm H}$)

The "He-burners" evolve at a somewhat lower luminosity, which could in principle be used to estimate their fraction in samples at the same distance (Galactic Bulge, Magellanic Clouds).

If the TP phase ϕ is close to 1 at the end of the AGB, the star may suffer a late thermal pulse during the post-AGB phase. Evolutionary calculations show that this can bring back the star to location of the AGB in the HR-diagram, and start a new phase of post-AGB evolution (see Fig. 39). These are known as "born-again AGB stars". That this is not just a theoretical construction is shown by a small number of objects, V605 Aql, FG Sge, V4334 Sgr ("Sakurai's Object"), which show rapid changes in their effective temperature, as well as in their atmospheric abundances.

These kind of late thermal pulses have also been proposed as the cause of H-deficient post-AGB stars. These stars have spectra similar to massive, C-rich Wolf-Rayet stars, and are designated as [WC]-stars[1]. These stars have almost no H, and very high He, C

[1]The square brackets indicate that their spectra show forbidden lines; these are produced in the CSE.

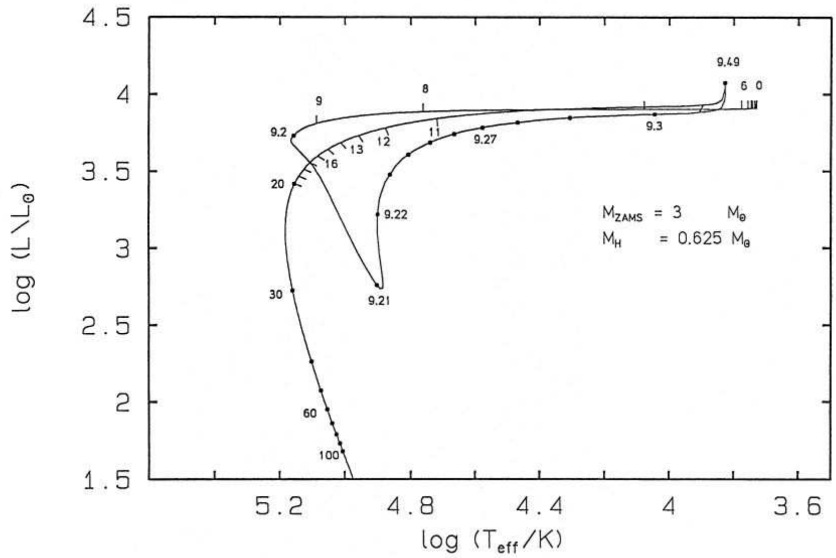

Fig. 14. Evolution of a post-AGB models with $(M_{\rm ZAMS}, M_{\rm H}) = (3M_\odot, 0.625M_\odot)$. Time marks are in units of 10^3 yrs ($\phi = 0.87$)

Figure 39: Stellar evolution calculations of a $M_{\rm ZAMS} = 3\ M_\odot$ star which undergoes a late thermal pulse ($\phi = 0.87$). Its final mass is 0.625 $M_\odot$. The times along the track are in units of 1000 years. From Blöcker (1995).

and O abundances. They also show much larger mass loss rates than normal post-AGB stars, which can be understood since line-driven mass loss mostly relies on metal lines. Once they have evolved in WDs, they are probably the so-called PG 1159 stars.

8.4 The circumstellar envelope during the post-AGB

The post-AGB evolution is rapid enough for the mass lost during the AGB to still be present around the star. All post-AGB stars are thus surrounded by circumstellar material (CSM), and it is often this CSM that makes these stars noticeable.
Two stellar effects modify the CSE during the post-AGB phase:

1. The changing stellar spectrum (as the star evolves from stellar type M via K, etc. to O).

2. The increase of the velocity of the stellar mass loss

As the star evolves through the various spectral types, its $T_{\rm eff}$ increases, and the spectrum hardens. UV photons start to destroy first the molecules, and then ionize the atoms. Traditionally the division line is places at $T_{\rm eff} = 3 \times 10^4$ K beyond which the star produces so much UV radiation that a substantial part of the CSE becomes ionized. The CSE then gets called a ***Planetary Nebula***.
At lower $T_{\rm eff}$ there is almost no, or very little ionization and then the objects are called ***Pre-Planetary Nebulae***, or proto-planetary nebulae[2], or transition objects.

8.4.1 Pre-Planetary Nebulae

Pre-Planetary Nebulae (PPNe) are a separate class of objects. Often the star itself is too deeply embedded to be directly observable. If the star is observable, its spectrum resembles that of supergiants. The reason for this is that the stellar atmosphere is still quite extended (so the surface gravity is low), and the stellar photosphere has temperatures that place it in the range of spectral types G, F, A. In fact the group of "high (galactic) latitude supergiants" are most likely all post-AGB stars, since it is unlikely that massive stars would form at high galactic latitudes.
The CSE in this phase is a strong IR source, requiring satellite data to study it. In some cases spectacular reflection nebulae are seen (Red Rectangle, Egg Nebula, Frosty Leo, etc, see Fig. 40). All of these are strongly aspherical, and some show signs of fast (~ 100 km s^{-1}) outflows.
The youngest PPNe are probably hard to separate observationally from AGB stars. For example, PPNe also sometimes show OH-maser emission, although not with the same thin shell-like morphology. Infrared spectroscopy (which first made possible with sufficient spectral resolution by the ISO mission) shows how the chemical composition of the CSE slowly starts to be modified because of the hardening radiation from the star. Certain molecules disappear, others form. The interpretation of these data require careful modelling using so-called *photo-dissociation* models.

[2]Confusion with proto-planetary discs is possible when using this name.

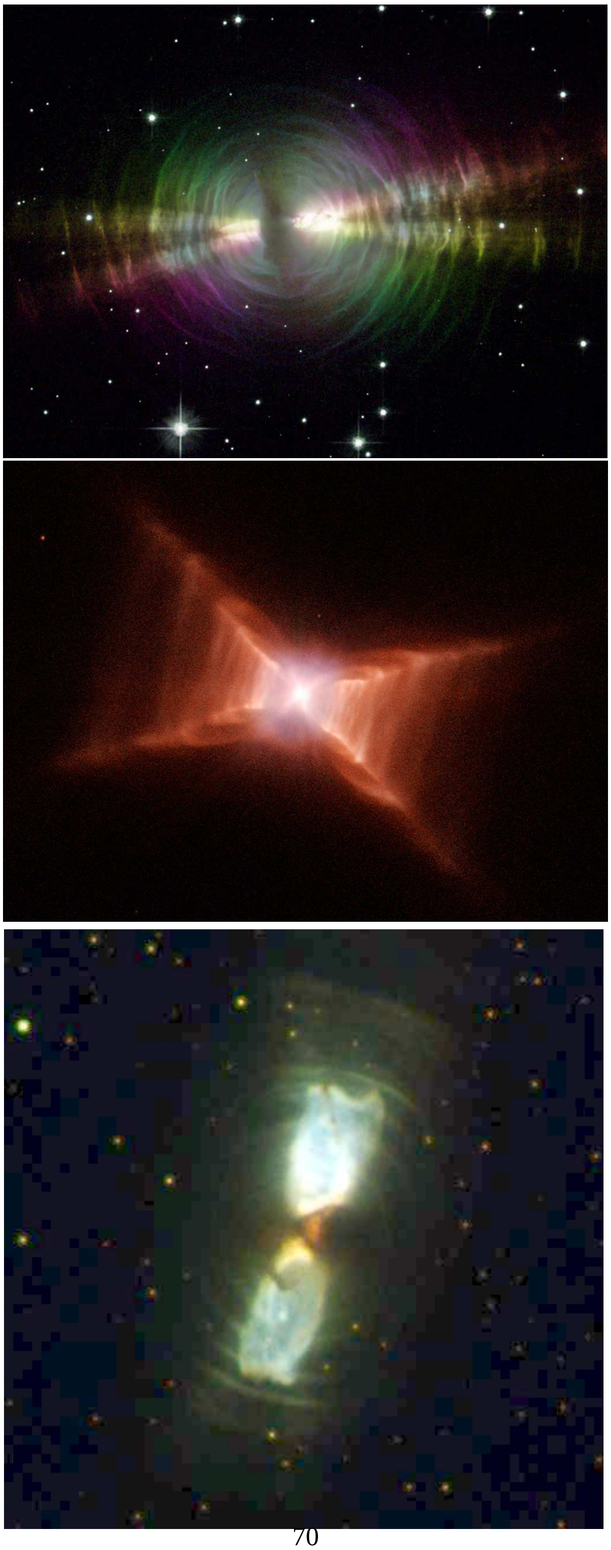

Figure 40: Three well known preplanetary nebulae objects, shown in optical scattered light: Egg Nebula (CRL 2688), Red Rectangle (HD 44179), Cotton Candy Nebula (IRAS 17150-3224).

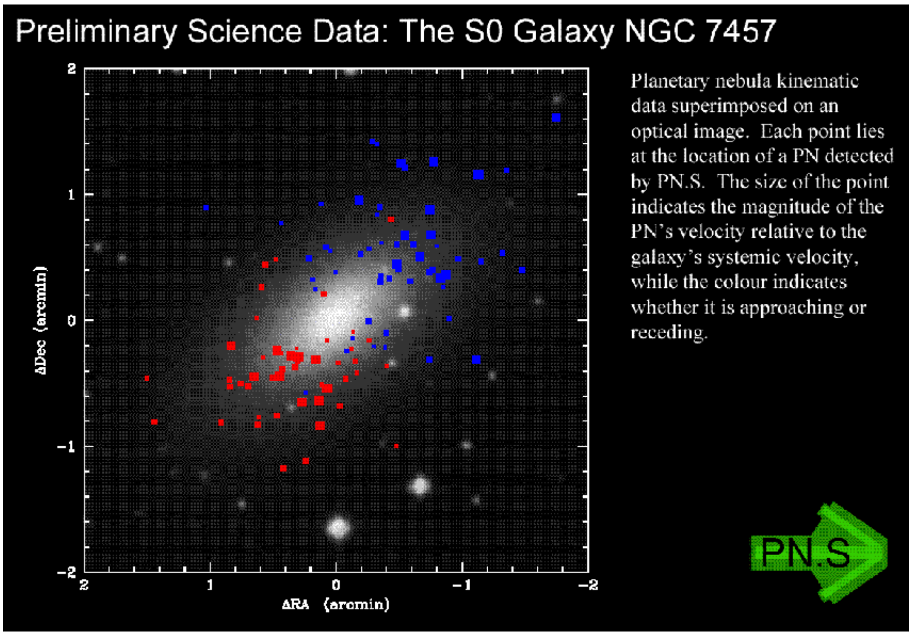

Figure 41: Overview of PNe detected in the galaxy NGC 7457 with the PN-spectrograph on the William Herschel Telescope.

8.4.2 Planetary Nebulae

Planetary Nebulae (PN, plural PNe) are characterized by emission from ions, and are normally found through their Hα and [OIII]5007Å emission. PNe are the only galactic objects that produce large quantities of O^{2+}, due to their very hard spectra. Due to the typical excitation properties a large fraction of the stellar light comes out in the line. This even makes it possible to detect PNe in other galaxies (see Fig. 41), using narrowband surveys. The Doppler shift of the line then allows one to study the galactic dynamics of these galaxies. In a similar way, PNe have been used as distance indicators by comparing luminosity function.

Due to the the continuing expansion of the CSE, PNe are rather large objects: 10^{17}—10^{18} cm, and therefore can even be imaged in the Magellanic Clouds (with the Hubble Space Telescope). Since the nebula emits mostly line emission, narrowband filters are often used for this (Fig. 42). Images in different lines are not always identical, indicating that the photon field changes as the radiation moves out through the nebula (see Fig, 43). PNe are traditionally seen as part of the Interstellar Medium (ISM), and textbooks on the ISM often include sections on PNe. The ISM course (AS7001) will address in detail the physics of ionized gasses.

The image data show very few PNe to be spherical ($\lesssim$ 10%), and a wide range of morphologies exist. One could claim that when imaged in detail, every PN is unique. Still, general patterns show up: elliptical shells, bipolar nebulae, point-symmetry (see

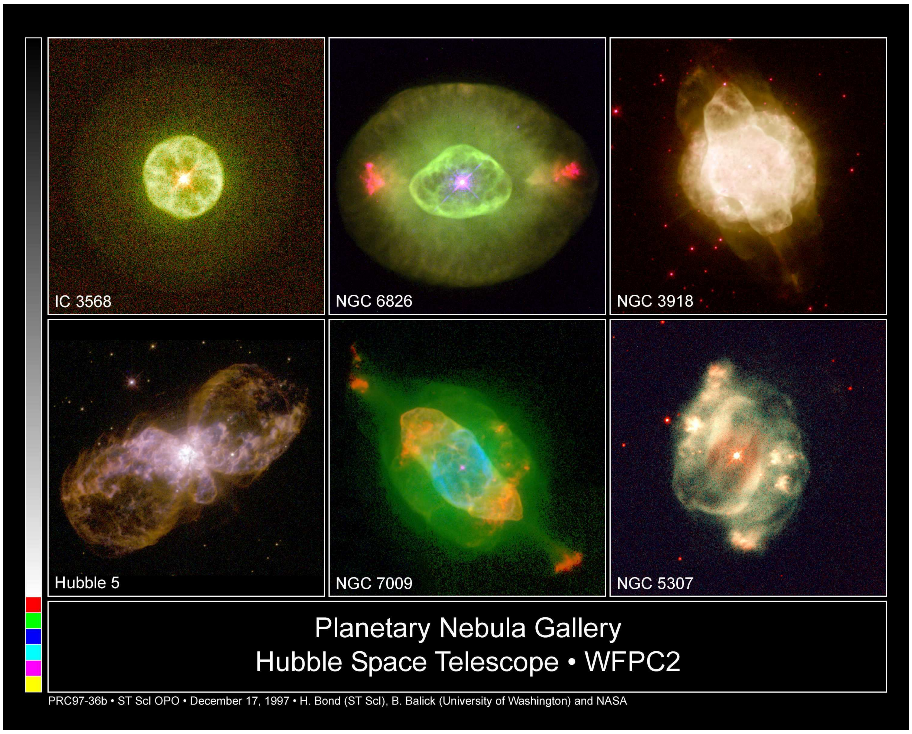

Figure 42: A collection of HST narrowband images of PNe, illustrating the wide range of morphologies found in PNe. The different colours correspond to different narrowband filters (but the colour coding and filters differ between images).

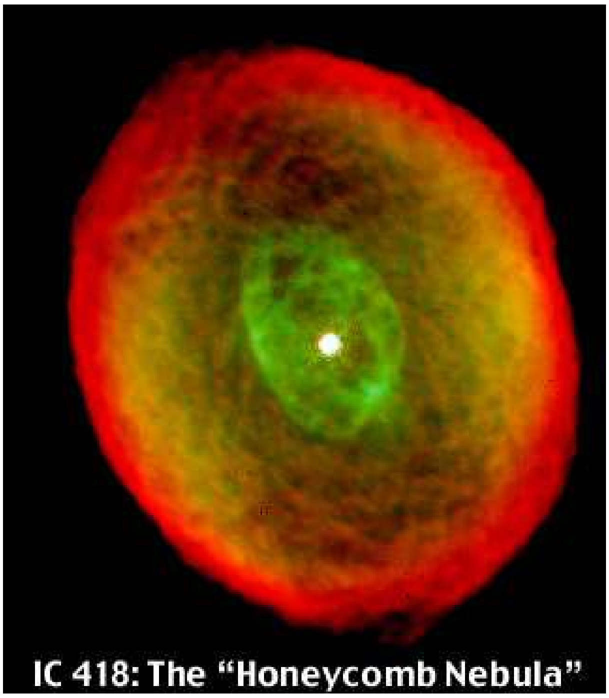

Figure 43: HST image of IC 418. Red is the [NII] filter, yellow the Hα filter, green the [OIII] filter. The outer bright edge may be an ionization front, whereas the inner green structure may be the windblown bubble.

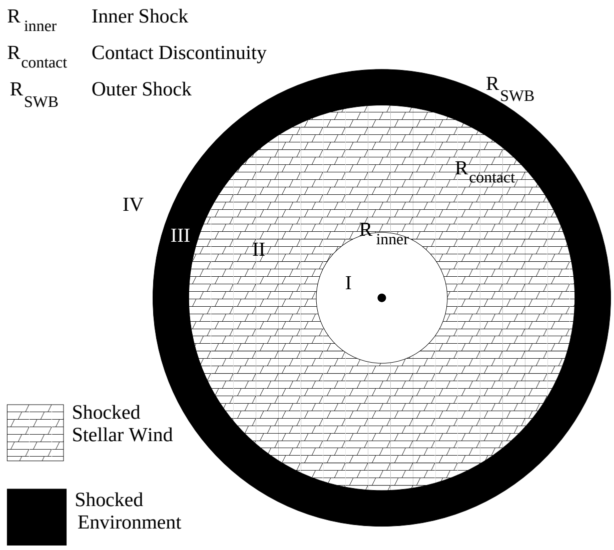

Figure 44: Schematic overview of a stellar wind bubble, such as found in PNe. See the text for a description.

for example Fig. 42).
Spectroscopy of high enough resolution can measure the expansion velocity of PNe. These fall in the range 20—100 km s^{-1}, depending on the object or the position inside the object. These velocities are higher than those around AGB star, pointing to the process of *interacting stellar winds* (ISW): the faster post-AGB wind (100s to 1000s of km s $^{-1}$) runs into the $\sim$ 10 km s $^{-1}$ AGB material and pushes it outward at a higher velocity.
A simple model of such a fast wind interacting with a slow wind (AGB mass loss) leads to a bubble structure (Fig. 44) with three discontinuities

$R_{\rm inner}$**:** inner shock

$R_{\rm contact}$**:** contact discontinuity

$R_{\rm outer}$**:** outer shock

and four regions

I: unshocked fast wind

II: shocked fast wind, low density, high ($\sim 10^7$ K) temperature; also known as the 'hot bubble'.

III: shocked slow wind: high density, nebular ($\sim 10^4$ K) temperature(mostly due to the stellar radiation); the PN shell.

IV: unshocked slow wind: high density (but lower than in region III), nebular temperature (due to the stellar radiation)

If region IV contains density variations, the shell (III) will become aspherical. This model can be used to explain the various morphologies seen in PNe.
The hot gas in region II emits X-ray radiation which has been observed in a number of PNe, showing that the ISW picture is valid (see Fig. 45).
As the PN expands it will merge with the ISM, carrying back stellar material to that may again be used for star formation. Due to the convective mixing and mass loss on the AGB this material will have become more enriched in elements. Also some of the dust particles formed around the AGB star survive the exposure to UV radiation and form the basis of the interstellar dust population.
Not all post-AGB stars will make a PN though. The post-AGB evolution of low mass stars ($\lesssim 0.5\ M_{\odot}$) is so slow (see Fig 38) that the CSE will have dispersed before the star becomes hot enough to ionize it.

8.4.3 Asphericity in the post-AGB phase

Observations of AGB stars do not show strong signs of aspherical mass loss, and yet asphericity is commonly seen in PPNe and PNe. Some of these objects show an aspherical shape inside more spherical structures (see Fig. 46). This suggests that the introduction of asphericity takes place at the very end of the AGB, or during the earliest post-AGB phases. However, the physical cause of this remains under debate. Probably some, or all of the following processes play a role:

- rotation
- magnetic fields
- binarity / planetary systems
- accretion discs

The cause of aspherical mass loss around the end of the AGB is perhaps the single most important unsolved problem in the evolution of low mass stars. The short time scales on which it becomes active, as well as the fact that it happens during the most embedded/obscured phase of AGB evolution, make it an extremely tough problem to solve.

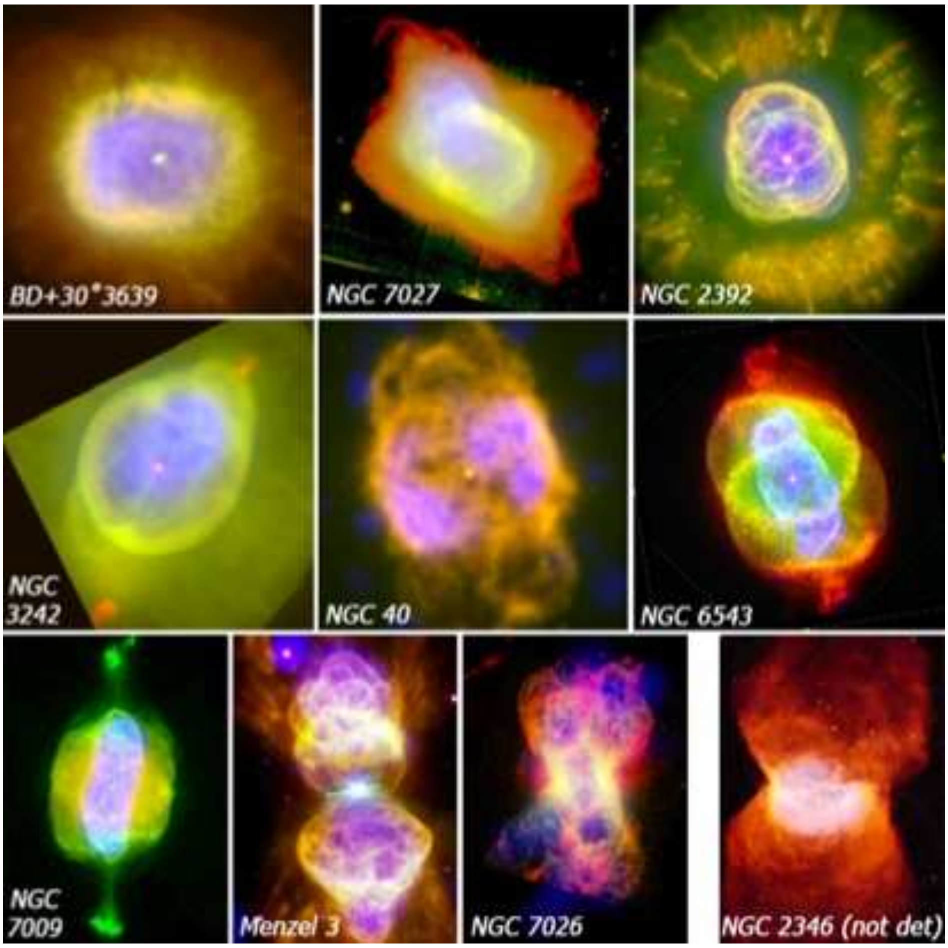

Figure 45: An overview of PNe in which extended X-ray emission has been detected (apart from NGC 246). The X-ray emission is shown in blue, the other colours indicate optical emission. From Kastner (2008).

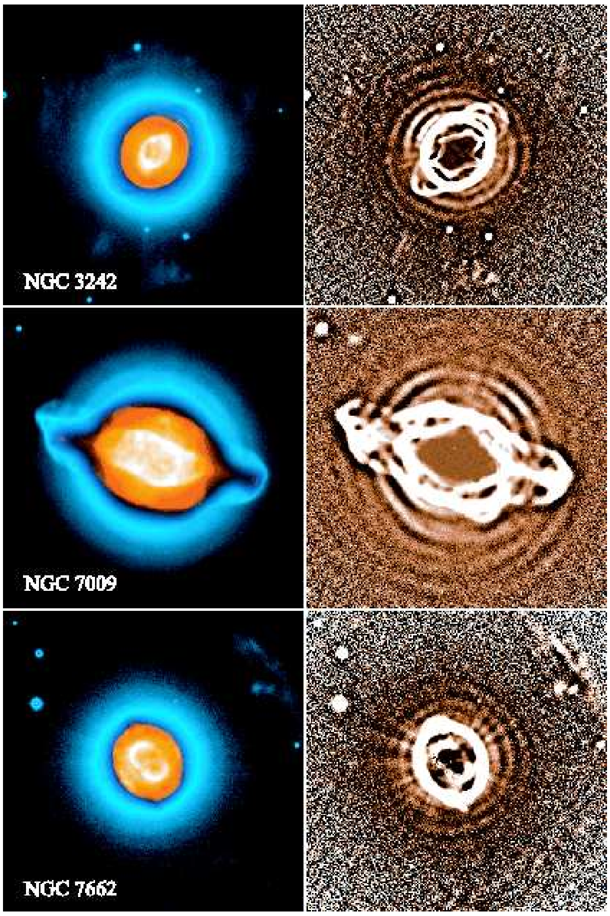

Figure 46: A collection of PNe showing (low surface brightness) spherical rings around their interior bright nebula. From Corradi et al. (2004).